CASE FILE COPY

NATIONAL ADVISORY COMMITTEE FOR AERONAUTICS

TECHNICAL NOTE 2981

THE HIGH-SPEED PLANING CHARACTERISTICS OF A RECTANGULAR FLAT PLATE OVER A WIDE RANGE OF TRIM

AND WETTED LENGTH

By Irving Weinstein and Walter J. Kapryan

Langley Aeronautical Laboratory Langley Field, Va.

JUL 27 1953



Washington July 1953

NATIONAL ADVISORY COMMITTEE FOR AERONAUTICS

TECHNICAL NOTE 2981

THE HIGH-SPEED PLANING CHARACTERISTICS OF A RECTANGULAR

FLAT PLATE OVER A WIDE RANGE OF TRIM

AND WETTED LENGTH

By Irving Weinstein and Walter J. Kapryan

SUMMARY

In order to extend the range of available planing data, the principal high-speed planing characteristics for a prismatic surface having an angle of dead rise of 0° (flat bottom) have been determined over a wide range of planing variables. Wetted length, resistance, center-of-pressure location, and draft were determined at speed coefficients ranging up to 25.0, beam loadings up to 87.3, and trims up to 30°. Mean wetted lengths up to 7.0 beams were obtained wherever possible. The data indicate that the important planing characteristics are independent of speed and load for a given trim and are dependent primarily upon lift coefficient. The ratio of center-of-pressure location forward of the trailing edge to the wetted length is a constant equal to 0.71 up to 9° of trim. This ratio decreases with a further increase in trim angle.

INTRODUCTION

The National Advisory Committee for Aeronautics has undertaken an experimental investigation of the high-speed planing characteristics of a series of related prismatic surfaces. The principal purpose of this investigation is to extend the available data to high speeds, high trims, and long wetted lengths. The results of tests of surfaces having angles of dead rise of 20° and 40° are presented in references 1 to 3.

The present paper presents the results obtained with a prismatic surface having an angle of dead rise of 0° (flat bottom). The principal planing characteristics were determined for speed coefficients up to 25.0, beam loadings up to 87.3, wetted lengths up to 7.0 beams, and trims up to 30°. The characteristics determined were wetted length, resistance, center-of-pressure location, and draft for suitable combinations of speed, load, and trim.

SYMBOLS

Ъ	beam of planing surface, ft
đ	draft at trailing edge (measured vertically from undisturbed water level), ft
F	friction, parallel to planing surface, lb
g	acceleration due to gravity, 32.2 ft/sec ²
l _m	mean wetted length, ft
$\iota_{\mathtt{p}}$	center-of-pressure location (measured forward of trailing edge), $\frac{M}{\Delta\cos\tau+R\sin\tau},\text{ft}$
М	trimming moment about trailing edge of model, ft-lb
Δ	vertical load, 1b
R	horizontal resistance, lb
R _e	Reynolds number, $V_m l_m / \nu$
S	principal wetted area (bounded by trailing edge, chines, and heavy spray line), sq ft
V	horizontal velocity, fps
V _m	mean velocity over planing surface, $\sqrt{V^2 \left(1 - \frac{C_{L_b}}{\frac{l_m}{b} \cos \tau}\right)}$
W	specific weight of water, lb/cu ft
\mathtt{C}_{\triangle}	load coefficient or beam loading, Δ/wb^3
$\mathtt{C}_{\mathtt{f}}$	$\frac{F}{\frac{\rho}{2} \text{ SV}_{\text{m}}^2} = \frac{\cos \beta \cos^2 \tau}{\frac{l_{\text{m}}}{b} \cos \tau - C_{\text{L}_{b}}} \left(^{\text{C}}_{\text{D}_{b}} - ^{\text{C}}_{\text{L}_{b}} \tan \tau \right)$

c_R	resistance coefficient, R/wb ³
C _V	speed coefficient or Froude number, V/\sqrt{gb}
$^{\mathrm{C}}\mathrm{L}_{\mathrm{D}}$	lift coefficient based on square of beam, $\frac{\Delta}{\frac{\rho}{2}V^2b^2} = 2\frac{c_{\Delta}}{c_{V}^2}$
c _{Db}	drag coefficient based on square of beam, $\frac{R}{\frac{\rho_{V} v_{b}^{2}}{2}}$
$c_{ m Ls}$	lift coefficient based on principal wetted area, $\frac{\Delta}{\frac{\rho}{2}v^2s} = \frac{c_{L_b}}{l_m/b}$
c_{DS}	drag coefficient based on principal wetted area, $\frac{R}{\frac{\rho}{2} v^2 s} = \frac{{}^C D_b}{l_m/b}$
β	angle of dead rise, deg
ρ	mass density of water, slugs/cu ft
τ	trim (angle between planing bottom and horizontal), deg
ν	kinematic viscosity, ft ² /sec

DESCRIPTION OF MODEL

The model used for this investigation had an angle of dead rise of 0° , a beam of 4 inches, and a length of 36 inches and was constructed of brass. A sketch and cross section of the model with its pertinent dimensions are shown in figure 1. The tolerances and the finish of the model were the same as those described in reference 1.

APPARATUS AND PROCEDURES

Langley tank no. 1, the apparatus for towing the model, and instrumentation for measuring the lift, drag, and trimming moment are described

NACA TN 2981

in reference 4. A diagram of the model and towing gear is presented in figure 2. The test procedures were similar to those described in references 1 and 2.

The wetted areas were determined from underwater photographs in the manner described in reference 1. Where photographs were not available, visual readings of the wetted length were used to determine the wetted areas. A typical underwater photograph is shown as figure 3. The wetted length $l_{\rm m}$ was measured from the trailing edge of the model to the intersection of the heavy spray line with the planing bottom. Because of a slight curvature of the heavy spray line, the wetted length at the center line was approximately 0.3 inch greater than that at the chine. An arithmetic mean value of this line, therefore, was used. This mean value corresponds closely to the value of the wetted length at one-quarter beam inboard of the chine, which was the point at which the wetted length was observed during the flat-plate investigation reported in reference 5.

Draft measurements were obtained by the method described in reference 2, where a vertically oscillating prod was used to measure changes in the water level. These changes were applied as corrections to visual draft readings. The prod was located slightly forward and to the side of the model (in the approximate location of the water-level indicator shown in fig. 7 of ref. 1). As mentioned in reference 1, a careful survey of the water surface indicated no appreciable gradient in height in the vicinity of the test area.

The aerodynamic forces on the model and towing gate were held to a minimum by the use of the windscreen described in reference 1. The residual windage tare for resistance amounted to only 0.3 pound at a speed of 82 feet per second. The proper tare was deducted from the drag measurements to obtain the hydrodynamic resistances. The tares for load and moment were found to be negligible. The quantities measured are believed to be accurate within the following limits:

Load, 1b														±0.15
Resistance, lb														
Trimming moment, ft-lb	•	٠		٠				۰	•					±0.50
Wetted length, in	٠				٠	•							۰	±0.25
Draft, in					•				٠					±0.05
Trim, deg					•									±0.10
Speed, fps		·												±0.20

RESULTS AND DISCUSSION

Presentation and discussion of data. The experimental data obtained in Langley tank no. 1 are presented in tables I and II in the form of

conventional nondimensional coefficients of the load, resistance, speed, wetted length, draft, and center of pressure. The lift and drag coefficients are presented in terms of both the square of the beam ($^{\rm C}{\rm L}_{\rm b}$ and $^{\rm C}{\rm D}_{\rm b}$) and the principal wetted area ($^{\rm C}{\rm L}_{\rm S}$ and $^{\rm C}{\rm D}_{\rm S}$). Data where the mean-wetted-length—beam ratios are less than 0.5 should be used with caution since the accuracy of measurement of such small wetted areas becomes marginal. The data presented in table II were obtained in the low-speed nonplaning range and are discussed more fully later in this report.

Plots of the data are presented in figures 4 to 13. The variation of mean-wetted-length—beam ratio $\it l_m/b$ with the lift coefficient $\it C_{L_b}$ is shown in figure 4. When plotted against $\it C_{L_b}$, the experimental data generally fall along a single curve for each trim. These trends are the same as those found for the surfaces having dead rise (refs. 1 to 3). In figure 5, the nondimensional center-of-pressure location $\it l_p/b$ is plotted against $\it C_{L_b}$. Figure 6 shows that, for practical purposes, the ratio $\it l_p/l_m$ is constant for each trim and varies from 0.71 at 2° trim to 0.59 at 30° trim. The variation of draft d/b with lift coefficient $\it C_{L_b}$ is shown in figure 7.

A comparison of the measured draft with that computed from the wetted length is presented in figure 8 where the measured draft is plotted against $\frac{l}{h}\sin \tau$. The wetted length l used in this figure is measured from the trailing edge of the model to the intersection of the heavy spray line midway between the chines and therefore corresponds to the keel wetted length $\,\mathit{l}_{k}\,$ of references 1 to 3. The purpose of these plots, as discussed in references 1 and 2, is to establish whether a pile-up of water occurred at the intersection of the planing plate with the free-water surface. At the higher trims, the measured draft was less than that computed from the wetted length and indicated a piling up of water under the planing surface. (See fig. 9(a).) Similar pile-up, but to a lesser degree, was noted for the surfaces with dead rise (refs. 1 to 3). At low trims, however, the measured draft was more than that predicted from measurements of the wetted length. This result is contrary to expectations and should be viewed with caution. Evidence of this phenomenon is also presented in reference 6, where the results of a photographic study of piled-up water conducted with a series of V-shaped wedges having different angles of dead rise were reported. These surfaces were dropped vertically into a tank of water, and the shape of the free-water surface was photographed by means of a high-speed motionpicture camera. According to section 4.1 of reference 6, the free-water surface to the side of the model is slightly depressed during the impact

NACA TN 2981

6

of a wedge having the low angle of dead rise of 10° . The possibility exists that during steady-state planing a similar depression of the water surface occurs and that at low trims it is of greater magnitude than the pile-up at the intersection of the model with the free-water surface. (See fig. 9(b).) Reference 7, in its discussion of the planing process, also suggests the possibility of such a depression.

The preceding discussion applies to conditions where this effect could be due to air compression in the restricted area near the intersection of the planing surface with the water. Inasmuch as the present tests were made with a windscreen, one would expect this effect to be minimized. The screen, however, was 1 inch above the water and might have permitted sufficient air flow for this "air compression" to occur.

The resistance data are presented in figure 10 as a plot of drag coefficient ${}^{\rm C}{\rm D}_{\rm b}$ against lift coefficient ${}^{\rm C}{\rm L}_{\rm b}$. The solid lines faired through the data represent the total drag whereas the dashed lines, defined by ${}^{\rm C}{\rm L}_{\rm b}$ tan τ , represent the induced drag. The difference between the solid and dashed lines represents the friction drag. At low trims the friction drag is a larger portion of the total drag than at the higher trims. At high trims, the induced drag exceeds the total drag and indicates an apparent negative friction force. At these high trims the volume of forward spray is large and appears to have high forward velocity with respect to the model. The relative velocity of the model in the region of forward spray therefore is effectively reversed so that the friction drag due to this spray acts in a direction opposite to that of the drag in the principal wetted area and thereby reduces the total drag.

In practice, this forward flow of water would be expected to be reduced by the air flow around the model. In order to observe this effect, a few runs were made with the windscreen removed. The volume of water thrown forward, the apparent velocity of this spray, and the area wetted by this spray were all reduced. For these conditions, the induced drag more nearly approximated the total drag. For practical application in the range covered by the present test, therefore, the friction forces may be considered negligible at the high trims as was found for the surfaces having dead rise (refs. 1 to 3). Removal of the windscreen, however, did not eliminate the apparent negative friction force; therefore, the assumption of negligible friction forces results in slightly conservative drag estimates. For the dead-rise surfaces, the loose spray had no appreciable forward motion and removal of the windscreen had no measurable effect on the friction force.

Data from tests of a $2\frac{1}{2}$ -inch-beam flat plate, obtained without the presence of a windscreen in Langley tank no. 2, also show that, at high

trims (above 12°), the total drag is slightly lower than the induced drag, as do the tabulated data of reference 8 for conditions above 12° of trim.

The variation of friction coefficient with Reynolds number is presented in figure 11 for trims of 2° , 4° , 6° , and 9° at which the friction drag represented a significant proportion of the total drag. Most of the coefficients for the lighter loads and lower Reynolds numbers (below 1 x 10°) were erratic because of the marginal accuracy. All conditions, therefore, where the precision of measurement changed the coefficient by more than 20 percent were deleted from this plot. The friction coefficients were calculated directly from the tabular data. The grouping of the data along the Schoenherr turbulent-flow line indicates that, at low trims and high Reynolds numbers, the friction drag can be calculated with reasonable accuracy by use of the Schoenherr equation (ref. 9). This condition is also true for surfaces having positive angles of dead rise (refs. 1 to 3).

As reported in references 1 to 3, some of the light-load, low-speed conditions at the lower trims did not fit the curves for which \mathcal{C}_{L_h} is the governing parameter. Accordingly, in a manner similar to that described in reference 1, an attempt was made to determine the limitation of the plots against C_{L_h} . Wetted lengths, therefore, were measured at low speeds into the speed and load region where $\,^{ extsf{C}}_{ extsf{L}_{ extsf{D}}}$ longer the governing parameter. These data are presented in figure 12 as a plot of $l_{\rm m}/b$ against ${\rm CL_b}$. These data are seen to depart from the curves of the collapsed data of figure 4 in a systematic pattern with load as parameter. The points at which these curves depart from the collapsed curves establish a minimum load for pure planing. Figure 13 presents a plot of these minimum load values for pure planing and was determined on the basis of 20-percent buoyancy since most of the affected data fell in this buoyancy range. The actual points of departure from the collapsed curves in figure 12 are included in figure 13 and are seen to be in good agreement with the curves based on 20-percent buoyancy and presented in figure 13. Therefore, the few conditions encountered during the remainder of this test for which buoyancy equaled at least 20 percent of the load have been deleted from table I and from the curves.

Comparison with other flat-plate data. The flat-plate data of other experimenters are compared with those of the present paper in figure 14. Curves are presented defining the variation of $C_{L_{\hat{D}}}$ with trim at meanwetted-length—beam ratios of 1 and 3 for the data obtained at the Stevens Institute of Technology (S.I.T.) and by Sambraus (refs. 10 and 8, respectively). A substantial amount of flat-plate data is also presented by Shoemaker, Locke, and Sottorf in references 11, 12, and 5,

respectively. Their data, however, do not cover the beam loading and Froude number range of the present test and therefore are not compared in figure 14. The curves representing the S.I.T. formula which do appear in figure 14, however, are partially derived from these data.

Reference 10 presents the results of an analysis of most of the available flat-plate planing data in the form of an empirical formula for computing lift. According to this analysis, the effects of buoyancy are negligible above a speed coefficient of approximately 12.5. The lift curves in figure 14, representing the S.I.T. analysis, therefore, were derived on the basis of a speed coefficient of 12.5. The calculated lift coefficients are less than those obtained in the present investigation. This difference may be due to the fact that the bulk of the data used in deriving the empirical formula were obtained at speed coefficients lower than 7.0.

The data of Sambraus (ref. 8) were obtained at speed coefficients up to 13.0 and at these higher speed coefficients the results are in good agreement with those of the present investigation.

CONCLUDING REMARKS

The results obtained from an experimental investigation of a planing surface having an angle of dead rise of 0° indicate that, during high-speed steady-state planing, the important planing characteristics for a given trim depend primarily on lift coefficient. For engineering purposes, the ratio of center-of-pressure location forward of the trailing edge to the mean wetted length can be considered a constant equal to 0.71 at trims up to 9°. This ratio decreases with a further increase in trim angle. The friction drag can be considered negligible at the trims tested above 12° so that, for these trims, as in the case with surfaces having positive angles of dead rise, the total hydrodynamic drag, for engineering purposes, can be considered equal to the induced drag of the surface.

Langley Aeronautical Laboratory,
National Advisory Committee for Aeronautics,
Langley Field, Va., May 29, 1953.

F

REFERENCES

- 1. Kapryan, Walter J., and Weinstein, Irving: The Planing Characteristics of a Surface Having a Basic Angle of Dead Rise of 20° and Horizontal Chine Flare. NACA TN 2804, 1952.
- 2. Blanchard, Ulysse J.: The Planing Characteristics of a Surface Having a Basic Angle of Dead Rise of 40° and Horizontal Chine Flare. NACA TN 2842, 1952.
- 3. Chambliss, Derrill B., and Boyd, George M., Jr.: The Planing Characteristics of Two V-Shaped Prismatic Surfaces Having Angles of Dead Rise of 20° and 40°. NACA TN 2876, 1953.
- 4. Truscott, Starr: The Enlarged N.A.C.A. Tank, and Some of Its Work. NACA TM 918, 1939.
- 5. Sottorf, W.: Experiments With Planing Surfaces. NACA TM 661, 1932.
- 6. Bisplinghoff, R. L., and Doherty, C. S.: A Two-Dimensional Study of the Impact of Wedges on a Water Surface. Contract No. NOa(s)-9921, Dept. Aero. Eng., M.I.T., Mar. 20, 1950.
- 7. Sedov, L. I.: Planing on a Water Surface. R.T.P. Trans. No. 2506, British Ministry of Aircraft Production (from Tech. Vosdushnogo Flota, No. 4-5, 1940).
- 8. Sambraus, A.: Planing-Surface Tests at Large Froude Numbers Airfoil Comparison. NACA TM 848, 1938.
- 9. Davidson, Kenneth S. M.: Resistance and Powering. Detailed Considerations Skin Friction. Vol. II of Principles of Naval Architecture, ch. II, pt. 2, sec. 7, Henry E. Rossell and Lawrence B. Chapman, eds., Soc. Naval Arch. and Marine Eng., 1939, pp. 76-83.
- 10. Korvin-Kroukovsky, B. V., Savitsky, Daniel, and Lehman, William F.: Wetted Area and Center of Pressure of Planing Surfaces. Preprint No. 244, S.M.F. Fund Paper, Inst. Aero. Sci. (Rep. No. 360, Project No. NR062-012, Office Naval Res., Exp. Towing Tank, Stevens Inst. Tech., Aug. 1949.)
- 11. Shoemaker, James M.: Tank Tests of Flat and V-Bottom Planing Surfaces. NACA TN 509, 1934.
- 12. Locke, F. W. S., Jr.: Tests of a Flat Bottom Planing Surface To Determine the Inception of Planing. NAVAER DR Rep. 1096, Bur. Aero., Dec. 1948.

TABLE I

EXPERIMENTAL PLANING DATA OBTAINED FOR A RECTANGULAR FLAT PLATE

LANGLEY TANK MODEL 282

Average kinematic viscosity = 14.75 x 10^{-6} ft²/sec; specific weight of tank water = 63.4 lb/cu ft

Trim,	СД	c^A	c _R	l _m	i _p	<u>d</u>	c ^r p	СЪр	c _{LS}	c _{Dg}
	8555533333336666657777777777777777777777	6.16 6.16 6.16 6.16 6.16 6.16 6.16 6.16	0 213140666221 140606231 140606231 140606231 140606231 140606331 1	707577700 94 000285779 00770000 72070008555270025 617004716556885642042842465553047 21 2 42 33 87 31 63 18 611 11 411 44311 74111 84541 4254	1.72 1.11 .506 1.97 .13 4.01 .2.30 .4.02 .3.37 .3	0.125 .075 .048 .045 .055 .055 .122 .130 .058 .060 .038 .145 .075 .338 .112 .060 .042 .130 .055 .075 .338 .112 .060 .042 .075 .055 .075 .055 .075 .055 .075 .055 .075 .055 .075 .055 .075	0.0456 0.0477 0.203 0.0453 0.0203 0.0453 0.0203 0.0456 0.0456 0.0456 0.0456 0.0456 0.0456 0.0466 0.0340 0.0701 0.0810 0.0901 0.08101	0.0113 .0163 .0034 .0048 .0127 .0024 .0019 .0018 .0198 .0110 .0025 .0030 .0286 .0116 .0055 .0039 .0030 .0257 .0257 .0257 .0257 .0257 .0257 .0257 .0257 .0257 .0257 .0257 .0257 .0257 .0257 .0259 .0114 .0055 .0034 .0163 .0055 .0034 .0163 .0055 .0034 .0055 .0038 .0129 .0146 .0055 .0039 .0124 .0163 .0055 .0038 .0125 .0056 .0118 .0055 .0056 .0118 .0056 .0118 .0056 .0118 .0057 .0056 .0056 .0056 .0056 .0056 .0056 .0056 .0056 .0056 .0056 .0056 .0056 .0057 .0056 .0056 .0056 .0057 .0056 .0056 .0057 .0056 .0056 .0056 .0056 .0056 .0056 .0056 .0056 .0057 .0056 .0056 .0057 .0056 .0057 .0056 .0057 .0056 .0057 .0056 .0056 .0056 .0056 .0056 .0056 .0057 .0056 .0057 .0056 .0056 .0056 .0056 .0056 .0056 .0056 .0057 .0056 .0056 .0057 .0056 .0056 .0057 .0056 .0056 .0056 .0056 .0057 .0056 .0056 .0057 .0056 .0057 .0056	0.021 .025 .031 .037 .031 .031 .012 .015 .033 .009 .009 .009 .015 .027 .028 .029 .010 .022 .009 .059 .059 .059 .055 .081 .058 .092 .084 .092 .094 .095 .095 .096 .096 .097 .096 .097 .096 .097 .096 .097 .096 .097 .096 .097 .096 .097 .097 .097 .098 .099 .099 .099 .099 .099 .099 .099	0.0052 0090 0051 0087 0054 0028 0047 0040 0041 0043 0047 0040 0041 0047 0036 0037 0045 0045 0045 0045 00150 00150 00162 0050

aConditions for which average kinematic viscosity = 14.2×10^{-6} ft²/sec

TABLE I - Continued EXPERIMENTAL PLANING DATA OBTAINED FOR A RECTANGULAR FLAT PLATE LANGLEY TANK MODEL 282

Trim,	C∆	C.V	c _R	l _m	$\frac{l_p}{b}$	<u>d</u> b	C _L _p	c _D b	C _{LS}	C _{DS}
9ª	0 .885533399995555555555555555555555555555	4.58 4.515 5.837 7.26 9.18 8.39 10.66 8.39 10.66 8.39 10.66 8.39 10.66 10	0 • 112 • 222 23 318 66 67 27 38 0 97 74 0 92 90 66 97 86 92 90 66 66 66 55 59 98 87 38 99 94 111 1111111111111111111111111111	0 • 31 • 60 • 60 • 60 • 60 • 60 • 60 • 60 • 6	0.28 .85 .77 .78 .20 .20 .20 .20 .20 .20 .20 .20	0.160 .082 .072 .020 .020	0.0811 .0452 .0203 .1254 .08297 .0456 .0456 .0456 .0459 .0459 .0459 .0459 .0459 .0800 .0800 .0800 .0800 .0800 .0800 .0800 .08490 .0800 .08490 .08000 .08000 .08000 .08000 .08000 .08000 .08000 .08000 .08000 .08000 .08000 .08000 .08000	0.0143 .0069 .0038 .01653 .0110 .0062 .0073 .0197 .0197 .0197 .0107 .0197 .0107 .010458 .0303 .0191 .01107 .0181 .01107 .0181 .01107 .0181 .01107 .0181 .0181 .019	0.1351338 .1938 .1338 .1522 .1533 .0949 .0958 .1347 .0459 .0959 .0958 .1349 .005767 .1453 .005767 .1253 .005767 .1253 .005767 .1253 .005767 .0	0.0238 0.0230 0.0211 0.0122 0.0189 0.0189 0.0102 0.0146 0.085 0.0200 0.0164 0.089 0.0145 0.0200 0.0188 0.0099 0.0145 0.0200 0.0188 0.0072 0.0165 0.0200 0.0088 0.0072 0.0179 0.0067 0.0081 0.0072 0.0091 0.0128 0.0067 0.0081 0.0072 0.0091 0.0128 0.0067 0.0081 0.0072 0.0091 0.0128 0.0067 0.0081 0.0072 0.0091 0.0128 0.0067 0.0081 0.0129 0.01

aConditions for which average kinematic viscosity = 14.2 x 10 -6 ft²/sec NACA

TABLE I - Continued EXPERIMENTAL PLANING DATA OBTAINED FOR A RECTANGULAR FLAT PLATE LANGLEY TANK MODEL 282

Trim, T, deg	c∆	cv	c _R	l _m b	b b	d b	c ^r P	c _{Db}	c _{LS}	c _{DS}
12 12 12 12 12 12 12 12 12 12 12 12 12 1	0 • 855 • 85 • 85 • 85 • 85 • 85 • 85 •	\$\\\\\\\\\\\\\\\\\\\\\\\\\\\\\\\\\\\\\	0.18 22399.513.495.478.698.11.1.2222.22.190.18 2.191.495.190.18.699.18.699.18.699.18.699.18.699.18.699.18.699.18.699.18.699.18.699.18.699.18.699.18.699.18.699.19.19.19.19.19.19.19.19.19.19.19.19.1	28 10 10 10 10 10 10 10 10 10 10	0.56 .70 .09 .26 .1.76 .22 .35 .23 .2.91 .2.06 .46 .23 .2.3 .2.3 .2.91 .2.06 .23 .2.11 .2.05 .2.3 .2.11 .2.05 .2.3 .2.11 .2.05 .2.05 .2.11 .2.05 .2.11 .2.05 .2.11 .2.05 .2.11 .2.05 .2.11 .2.05 .2.11 .2.05 .2.11 .2.05 .2.11 .2.05 .2.11 .2.05 .2.11 .2.05 .2.11 .2.05 .2.11 .2.05 .2.11 .2.05 .2.11 .2.05	0.122 .042 .028 .608 .850 .180 .785 .532 .532 .518 .590 .375	0.0825 .0471 .0225 .02471 .0225 .02472 .1835 .1835 .08459 .0816 .07486	0.0175 .0122 .0061 .0029 .0592 .0370 .0422 .0171 .0101 .0165 .0085 .0947 .0257 .0159 .0083 .0047 .0532 .0385 .0290 .0291 .0227 .0151 .0087 .0760 .0538 .0247 .0152 .0165 .0538 .0247 .0170	0 - 295 - 314 - 225 - 197 - 229 - 229 - 2305 - 2305	0.0624 .0813 .0610 .0474 .0461 .05613 .0611 .0589 .0589 .0589 .0589 .0589 .0589 .0589 .0589 .0588 .0315 .0598 .0589 .0588 .0315 .0588 .0589 .0588 .0589 .0588 .0589 .0588 .0589 .0588 .0589 .0588 .0589 .0588 .0589 .0588 .0589 .0588 .0589 .0588

^aConditions for which average kinematic viscosity = 14.2×10^{-6} ft²/sec

TABLE I - Continued

EXPERIMENTAL PLANING DATA OBTAINED FOR A RECTANGULAR FLAT PLATE

LANGLEY TANK MODEL 282

Trim,	c _v	СV	c _R	l _m	l _p	d b	c ^{LP}	c _D _p	c _{LS}	c _{DS}
18 18 8 8 8 8 8 8 8 8 8 8 8 8 8 8 8 8 8	0.85 85 85 85 85 85 85 85 85 85 85 85 85 8	4.58 4.61 6.10 3.12 4.82 7.20 9.67 7.21 10.13 12.69 9.30 10.83 15.49 9.30 10.83 15.49 9.30 10.83 15.49 9.30 10.83 12.50 12.50 12.50 12.50 13.69 14.60 16.83 15.49 16.80 16.80 16.80 16.80 17.65 16.80 17.65 16.80 17.65 16.80 17.65 16.80 17.65 16.80 17.65 16.80 17.65 16.80 17.65 17.65 17.65 18.69 18.69 18.69 18.69 18.69 18.69 19.80 19.80 10.83	0.2607.44.900056884.66.335.55.55.55.55.55.58.87.88.79.88.87.33.33.33.33.33.33.33.33.33.33.33.33.33	0.18 .100	1.169.40 .829.1109.06551.88 .829.1109.06551.	0.045 	0.0810 0.0800 0.08507 0.08507 0.08507 0.08537 0.08537 0.08537 0.08567 0.08567 0.08567 0.08567 0.08567 0.08567 0.08575 0.085	0.0248 .0282 .0146 .0368 .0847 .0593 .0268 .0128 .0244 .0368 .0227 .0364 .0368 .0227 .0460 .0752 .07560 .0250	0. 45620667642421888733242776419910084680337639359066916672099712662336177633334445084444803376394672099712662336177633344450844445084444444444480977639467209971266236617760317783334445084444508444444444444849776778444444444444444444	0.1378 1567 11467 11467 11246 11317 11489 11280 11840 11840 11840 11840 1199 1106 1106 1107 1107 1108

TABLE I - Concluded

EXPERIMENTAL PLANING DATA OBTAINED FOR A RECTANGULAR FLAT PLATE

LANGLEY TANK MODEL 282

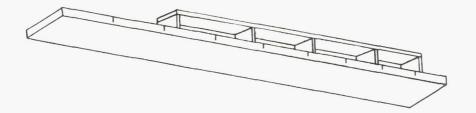
Trim, t, deg	С _Д	cv	c _R	l _m b	lp b	d b	СГР	СЪР	c _{LS}	c _{Ds}
444444444444444444444688888888888888888	27.69 27.69 27.69 36.21 36.21 36.22 53.22 553.22 553.22 553.22 553.22 70.29 87.33 87.33 87.33 87.33 87.33 10.65 11.17 11	15.01 17.45 21.11 11.90 13.42 14.88 20.94 14.49 16.16 18.39 20.77 20.86 24.40 16.59 20.92 24.61 18.54 20.62 23.33 24.95 5.68 10.13 12.78 9.67 12.41 17.45 21.72 14.91 17.45 20.86 24.98 11.99 13.24 14.98 24.98 11.99 13.24 14.98 24.99 11.99 13.24 14.98 24.99 11.99 13.24 14.98 24.99 11.99 13.24 14.99 13.24 14.99 13.24 14.99 13.24 14.99 13.24 14.99 13.24 14.99 13.24 14.99 13.24 14.99 13.24 14.99 13.24 14.99 13.24 14.99 13.24 14.99 13.24 14.99 13.24 14.99	11.66 11.53 11.35 15.68 15.68 15.68 15.68 15.68 15.68 15.68 15.68 15.68 15.68 15.68 16.22.77 22.43 22.24 21.71 30.94 22.28 22.24 21.71 30.95 37.50 37.52 38.01 37.50 37.52 38.01 37.56 10.73 10.36 10.37 10.36 10.36 10.36 10.36 10.36 10.36 10.36 10.37 10.36 10.37 10.36 10.36 10.37 10.	0.50 .32 .22 .75 .73 .32 .71 .00 .55 .32 .72 .74 .28 .75 .75 .30 .75 .75 .30 .75 .75 .75 .75 .75 .75 .75 .75 .75 .75	0.15738 0.15738 0.163 0.163 0.160	0.185	0.2458 .1819 .1243 .5114 .4021 .3271 .1803 .5072 .4078 .3150 .2469 .2469 .2469 .1800 .1787 .5108 .3212 .5081 .4108 .3209 .2806 .4104 .1955 .1245 .0782 .4104 .1955 .12489 .1234 .0813 .2491 .1819 .1234 .0888 .5038 .4131 .3227 .5072	0.1036 .07555 .0510 .2234 .1741 .1390 .0746 .2206 .1744 .1326 .1033 .0751 .0752	0 + 5659 3 7 3 7 9 8 4 8 4 4 7 7 5 3 7 9 7 7 6 6 9 8 1 4 5 7 7 3 9 8 4 8 4 5 7 5 7 5 1 5 5 5 7 8 1 4 5 7 9 8 1 4 5 7 5 1 8 6 7 1 1 4 5 9 1 4 6 6 8 8 8 1 8 1 8 1 8 1 8 1 8 1 8 1 8 1	0.2072 23759 2318 1831 1833 1986 2331 1737 1744 2276 1977 2272 1921 1974 2227 1813 1813 1969 2175 3487 3487 3564 3487 3564 2877 362 4062 4058 2848 3140 3270 2895

TABLE II

SUPPLEMENTARY EXPERIMENTAL DATA OBTAINED AT LOW SPEEDS FOR LANGLEY TANK MODEL 282

Average kinematic viscosity = 14.2×10^{-6} ft²/sec; specific weight of tank water = 63.4 lb/cu ft

Trim, , deg	СД	C∜	CR	i _m	l _p	c ^r P	СД	c _L _S	c _{DS}
++++++++6666666666669999999999999999	4.26 4.26 4.26 4.26 4.26 6.39 6.39 6.39 6.39 6.39 10.65	5550994599078886296658271426077088889114444555566677	0.92 1.000 1.94 1.44 1.11 1.15 1.18 2.002 2.001 2.097 3.73 1.097 1.175 1.288 1.175 1.266 2.001 2.092 2.094	8 77768 7778 8 7776 5 8 8 776 8 6 6 5 6 6 6 5 5 4 7 6 6 5 5 5	28159458568677791762696444125309 444455454443355444553344411920064	0.2116 .1926 .1844 .1744 .1542 .1830 .1652 .1576 .1644 .4100 .3572 .3060 .2666 .2404 .3146 .3120 .2984 .2700 .2512 .2980 .6020 .5280 .5170 .44530 .4480 .3640 .5192 .4640 .4230 .3920	0.0456 .0452 .0398 .0392 .03412 .0372 .0378 .0714 .0544 .0514 .05564 .0564 .0564 .0564 .0580 .1064 .1028 .0982 .1056 .1038 .0982 .1056 .0820 .0982 .0980 .0980 .0980 .0980 .0980 .0980	0.024 .024 .0224 .0222 .0222 .0222 .0222 .0349 .0442 .0441 .0439 .0339 .0340 .039 .0396 .0966 .0888 .087 .0867 .076 .0774	0.0055 .0057 .0053 .0056 .0055 .0049 .0049 .0045 .0083 .0075 .0082 .0075 .0074 .0074 .0074 .0074 .0074 .0074 .0074 .0074 .0074 .0074 .0069 .0167 .0166 .0167 .0168 .0161 .0169 .0150 .0150 .0150



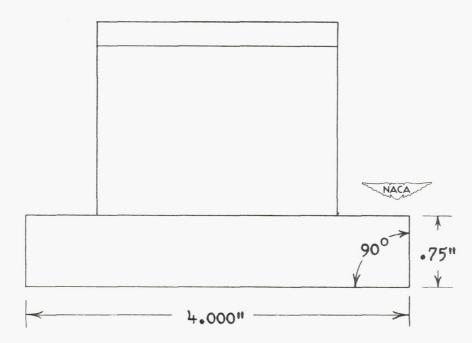


Figure 1.- Sketch and cross section of flat-plate model.

F

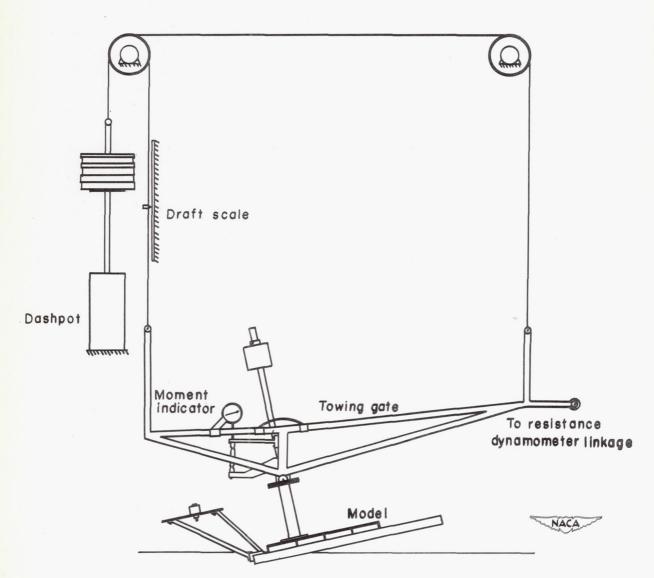


Figure 2.- Setup of model and towing gear.

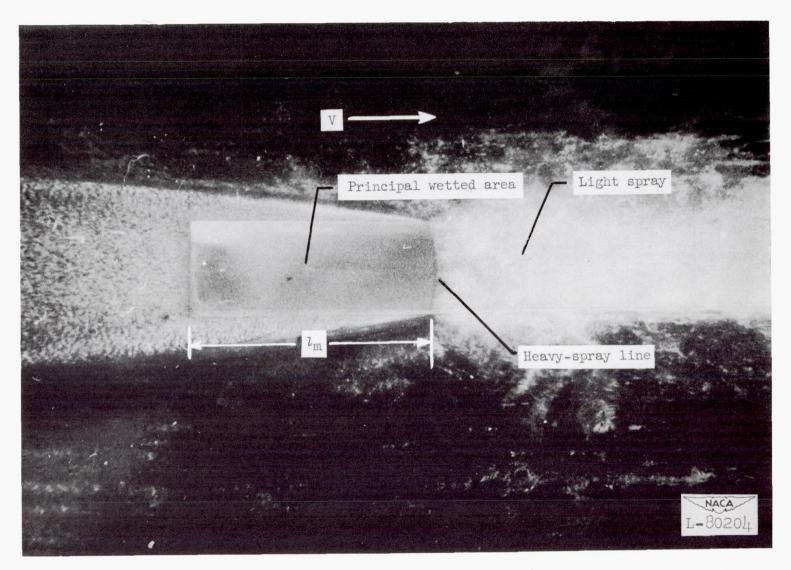


Figure 3.- Typical underwater photograph.

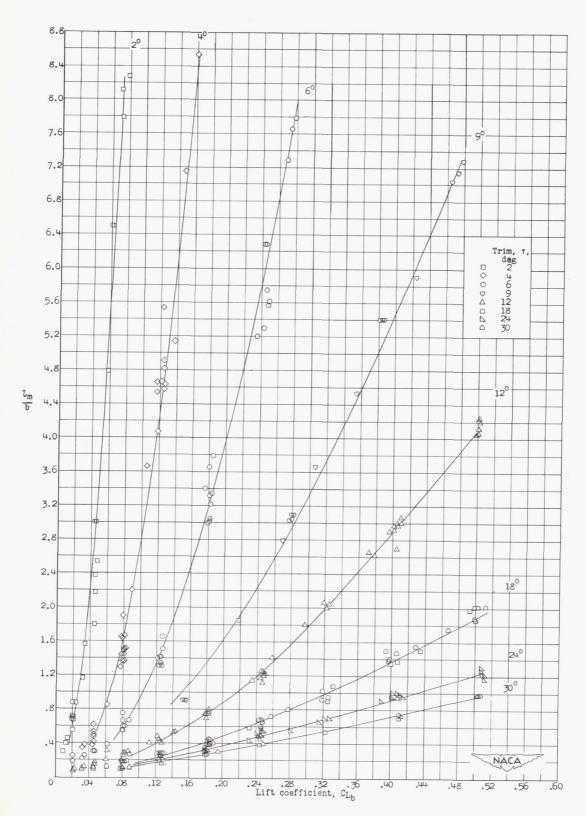


Figure 4.- Variation of mean-wetted-length—beam ratio with lift coefficient.

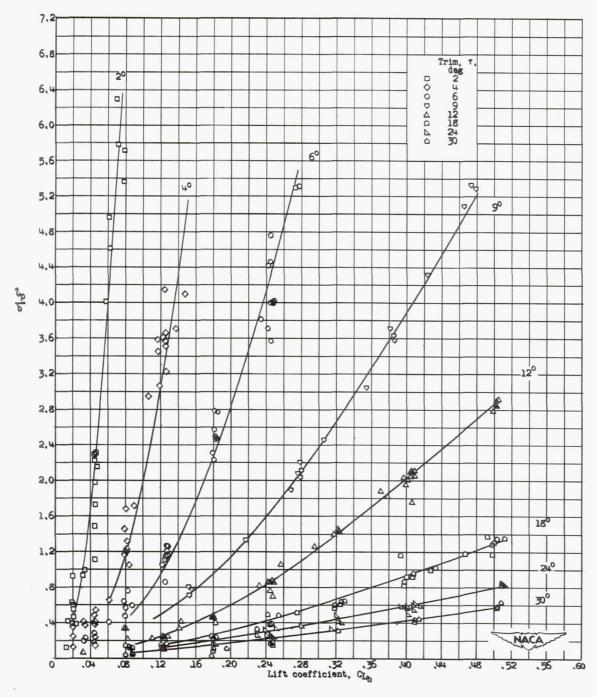


Figure 5.- Variation of nondimensional center-of-pressure location with lift coefficient.

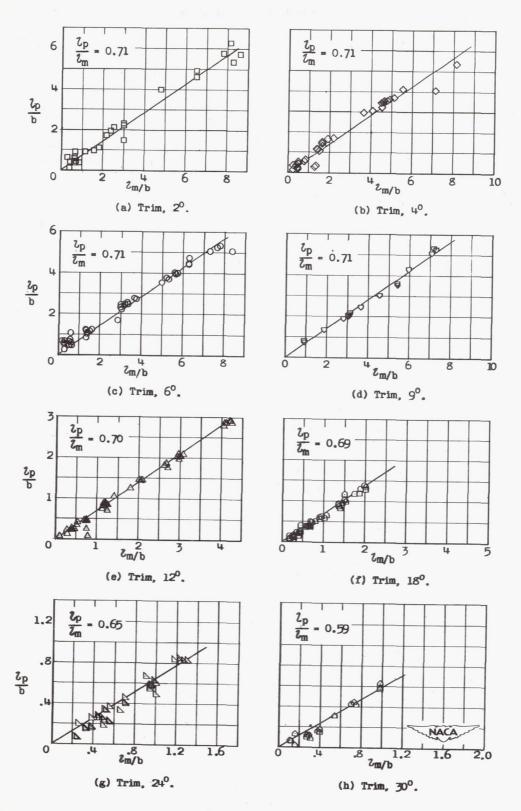


Figure 6.- Variation of center-of-pressure ratio with mean-wetted-length—beam ratio.

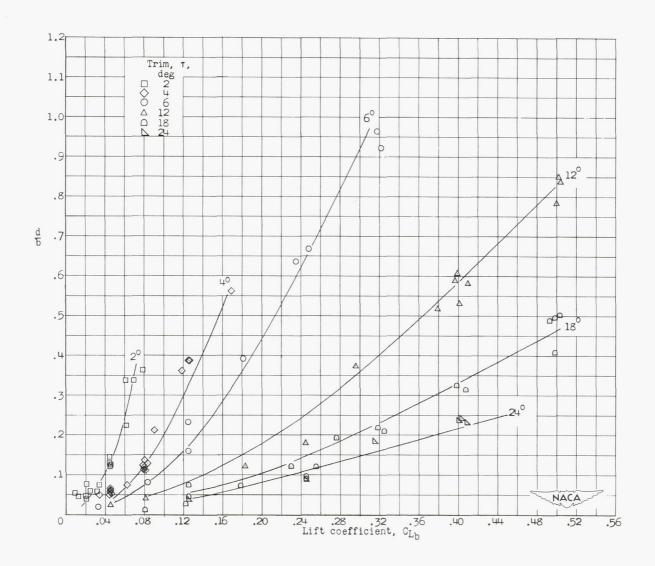


Figure 7.- Variation of draft with lift coefficient.

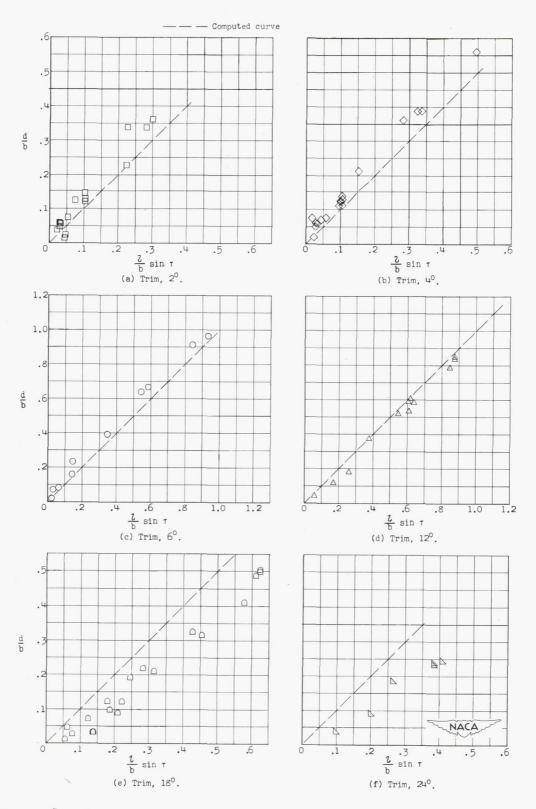
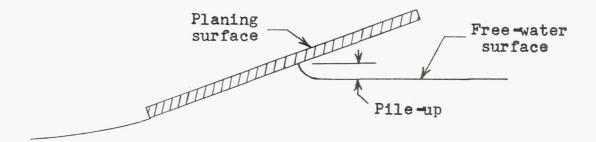
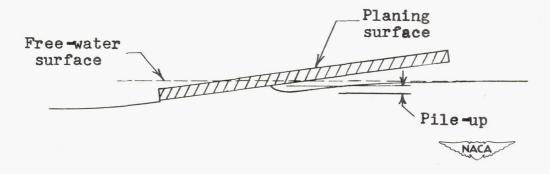


Figure δ .- Comparison of experimental draft data with computed curve.



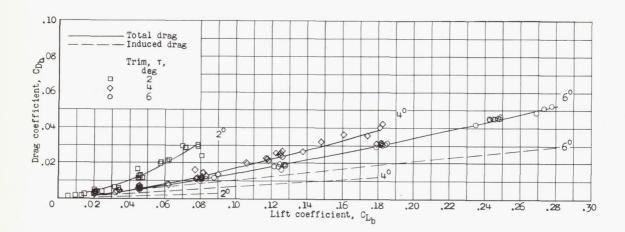
(a) Flow pattern at moderate and high trims.



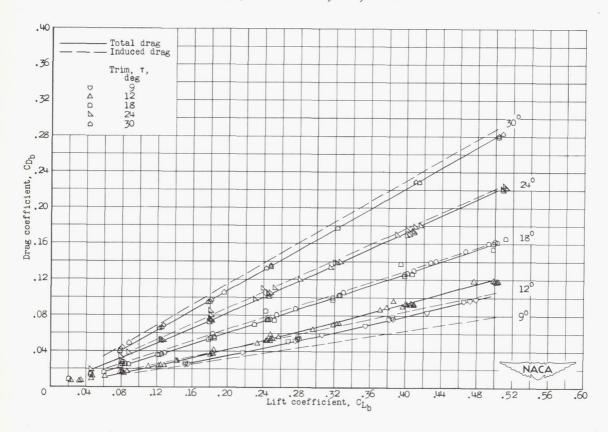
(b) Flow pattern at low trims.

Figure 9.- Sketches showing flow pattern at intersection of model with the water surface.

F



(a) Trim: 2° , 4° , and 6° .



(b) Trim: 9° , 12° , 18° , 24° , and 30° .

Figure 10.- Variation of drag coefficient with lift coefficient.

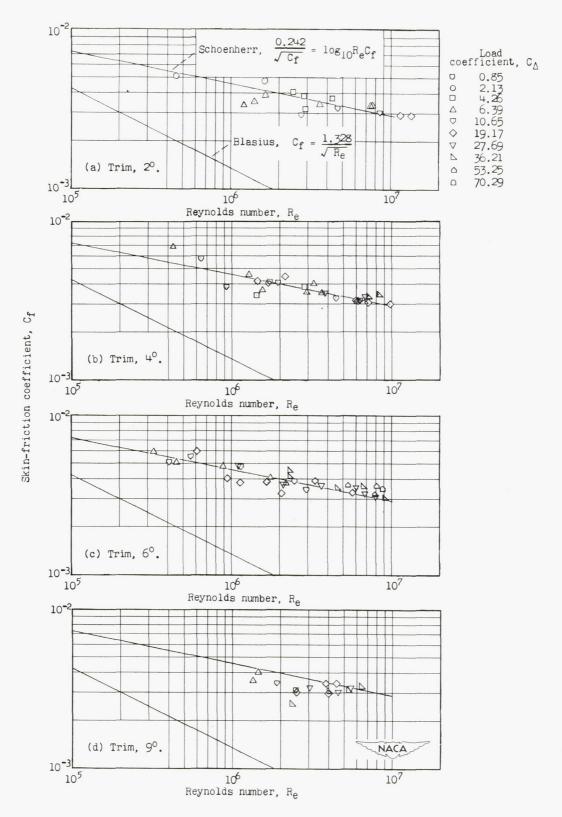


Figure 11.- Variation of skin-friction coefficient with Reynolds number.

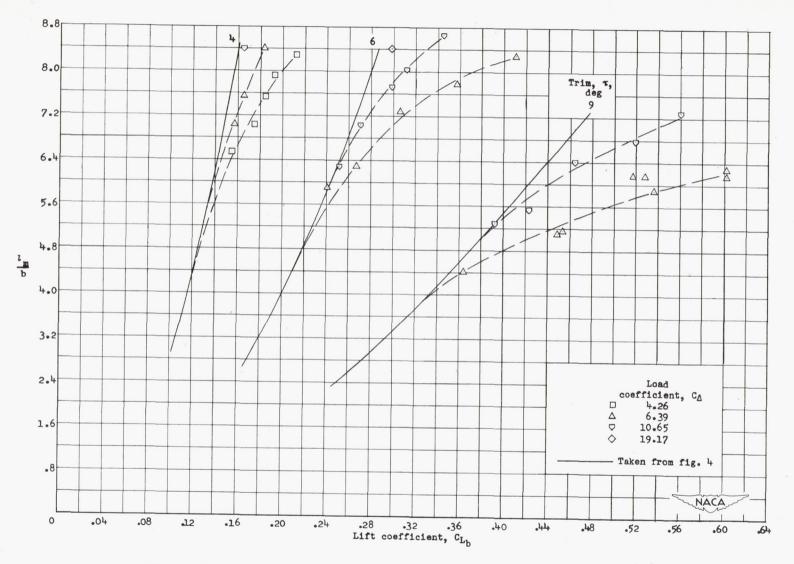


Figure 12.- Variation of mean-wetted-length—beam ratio with lift coefficient at low speeds.

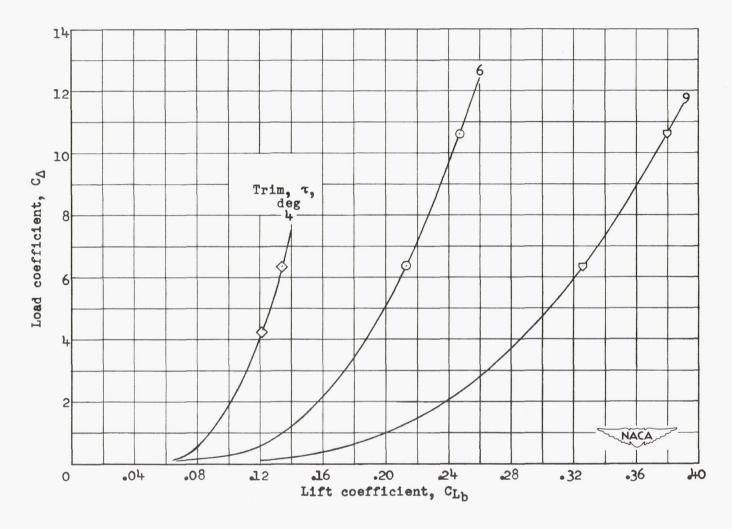


Figure 13.- Variation of minimum load coefficient for pure planing, based on 20-percent-buoyancy and test data.

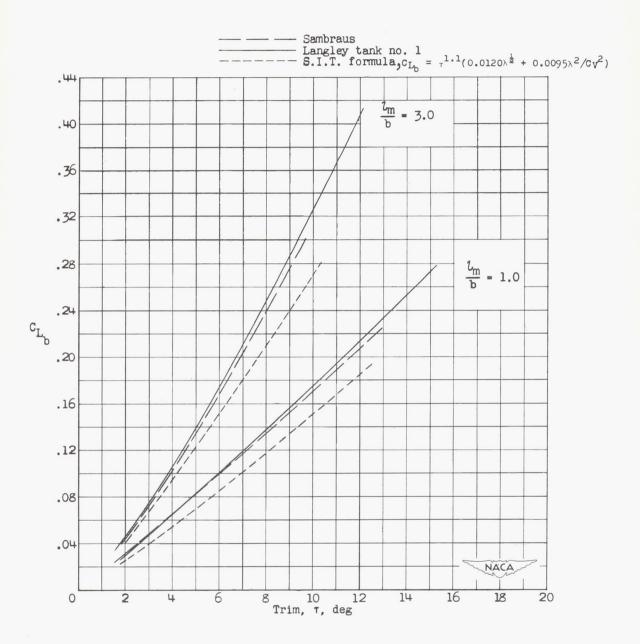


Figure 14.- Variation of lift coefficient with trim; comparison with data of other experimenters.